American Mineralogist, Volume 76, pages 501–511, 1991

Mg- and Cr-rich staurolite and Cr-rich kyanite in high-pressure ultrabasic rocks (Cabo Ortegal, northwestern Spain)

José I. Gil Ibarguchi, Miren Mendia
Departamento de Mineralogía-Petrología, Universidad del País Vasco–E.H.U., Aptdo. 644, 48080 Bilbao, Spain
Jacques Girardeau
Laboratoire de Pétrophysique, Université Paris VII–I.P.G. Paris, 2 Place Jussieu, 75230 Paris Cedex 05, France

Abstract

Metamorphosed ultrabasic rocks, likely derived from cumulate protoliths, occur intercalated within eclogites in the Cabo Ortegal complex (northwest Spain). Mg- and Cr-rich staurolite coexists with Cr-rich kyanite in these rocks. The staurolite has $X_{Mg} > 0.74$ and contains >6 wt% Cr_2O_3, and kyanite contains >4 wt% Cr_2O_3. Associated minerals are tschermakitic- to magnesio-hornblende, garnet, and zoisite. Mg- and Cr-rich staurolite and Cr-rich kyanite were formed through reactions involving partial destruction of Cr-rich spinel. Green pleochroism in staurolite and blue pleochroism in kyanite presumably result from Cr substitution for Al in the octahedral sites of these minerals. This substitution accounts for Cr enrichment in both minerals. Staurolite has greater affinity for Cr relative to Al than kyanite. In both there is, however, a significant difference between observed and ideal Al = Cr substitution. Mg enrichment in staurolite is controlled by cation substitution involving $^{[4]}$Fe sites. X_{Mg} values of staurolite, although showing considerable variation, may be as high as those of associated garnets but are consistently lower than those of associated amphibole ($X_{Mg} > 0.9$). Although the Cr contents of kyanite and staurolite could result from the Cr-rich bulk composition, the occurrences of small, colorless, Cr-poor kyanite included in matrix minerals and of blue, Cr-rich, matrix kyanite suggest increasing Cr substitution in kyanite with increasing pressure and temperature.

Introduction

Staurolite most typically occurs as an Fe-rich variety, commonly with kyanite, in pelitic rocks metamorphosed at intermediate pressures (4–6 kbar). However, staurolite also is found in higher pressure environments. It occurs with kyanite in intermediate- to high-pressure (8–12 kbar) metamorphosed basic and ultrabasic rocks (e.g., Selverstone et al., 1984; Ward, 1984; Nicollet, 1986; Helms et al., 1987). Moreover, as shown by experimental and field studies, staurolite in Mg- and Al-rich metamorphic rocks formed under high pressures and intermediate to high temperatures is enriched in Mg (Hellman and Green, 1979; Grew and Sandiford, 1984; Schreyer et al., 1984; Smith, 1984; Ward, 1984; Nicollet, 1986; Chopin, 1987; Enami and Zang, 1988; Schreyer, 1988). Staurolite is characteristically lower in X_{Mg} [= Mg/(Mg + Fe)] than coexisting silicate minerals; however, reversals in Fe-Mg partitioning (staurolite vs. garnet) have been reported from Mg-rich bulk-rock compositions (Nicollet, 1986; Schreyer et al., 1984; Enami and Zang, 1988) and proposed on the basis of staurolite solution models by Holdaway et al. (1988). High Cr contents in staurolite do not appear to be related to any specific *P-T* conditions, as they have been reported from high-pressure, magnesian (Nicollet, 1986) and medium-pressure, Fe-rich environments (Demange, 1976; Ward, 1984). Cr content is considered to be responsible for the green color of this mineral (Ward, 1984).

Although Cr content in kyanite has been shown experimentally to increase with increasing pressure (Seifert and Langer, 1970), reported Cr contents from kyanite coexisting with staurolite are not particularly high in basic and ultrabasic rocks metamorphosed to high pressure (Selverstone et al., 1984; Ward, 1984; Nicollet, 1986; Helms et al., 1987). Cr-rich kyanites have been reported only from basic and ultrabasic rocks without staurolite (Sobolev et al., 1968; Cooper, 1980).

In the course of the petrological study of eclogites and granulites from the Cabo Ortegal complex (northwest Spain), it has been found that some Mg- and Al-rich eclogites contain yellow staurolite with moderate Mg content (X_{Mg} of ca. 0.35), whereas green, Mg- and Cr-rich staurolite ($X_{Mg} > 0.74$, >6 wt% Cr_2O_3) and blue, chromian kyanite (>4 wt% Cr_2O_3) occur in hornblende-garnet-zoisite-kyanite-staurolite rocks of ultrabasic composition intercalated within eclogites with MORB composition. (We mean mineral color in thin section.) This is the most Cr-rich natural staurolite reported as far as we know, although X_{Mg} values are comparable to those of the most Mg-rich staurolite so far recorded in metamorphosed basic or ultrabasic rocks (Enami and Zang, 1988; X_{Mg} = 0.737 as average). Staurolite with higher X_{Mg} ratio has

0003–004X/91/0304–0501$02.00

only been found as rare inclusions within pyrope crystals in metasediments (magnesian metapelites) of the Dora Maira massif (western Alps, Chopin, 1987; 80–95 mol% end-member). The kyanite analyzed represents the most Cr-rich kyanite found in regionally metamorphosed rocks. Kyanite with higher Cr contents is known only in grospydite xenoliths from kimberlites (Sobolev et al., 1968). The results of the petrological and mineralogical study of the kyanite- and staurolite-bearing rocks from the Cabo Ortegal complex are described herein, and petrogenetic implications in the context of the metamorphic evolution of the complex are discussed.

Geologic setting

A geologic map of the northwestern part of the Iberian Massif shows the thrust stacking of a number of geologic units with different lithologic and tectonometamorphic characteristics. The uppermost thrust sheet crops out in the inner part of the Cabo Ortegal complex (Fig. 1). In this area it consists mainly of high-pressure/high-temperature (garnet-clinopyroxene) granulites, metaperidotites/pyroxenites, and eclogites (Fig. 1; Arenas et al., 1986; Gil Ibarguchi et al., 1990). The kyanite-staurolite-bearing rocks studied here occur within the eclogites. Synchronous granulitic and eclogitic events have been dated at ca. 480 Ma, the basic granulite protoliths being penecontemporaneous with the high-grade episode (Peucat et al., 1990). *T-P* conditions during these events were of ca. 800 °C, 13.5 kbar for granulites and similar temperatures and >17 kbar for eclogites (Gil Ibarguchi et al., 1990). Important retrograde recrystallization associated with ductile deformation under amphibolite-facies conditions has been dated at ca. 390 Ma (Peucat et al., 1990).

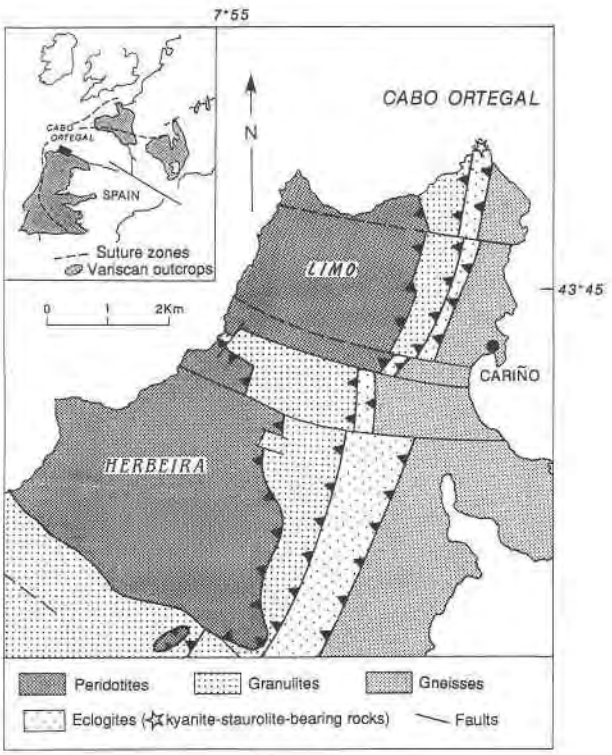

Fig. 1. Schematic geologic map of the northern part of the Cabo Ortegal complex with the location of the kyanite-staurolite-bearing rocks (barbs are on the upper plate of thrust faults). Inset: position of the Cabo Ortegal complex within the context of the Variscan Orogen.

Sample description

The eclogites at the Cabo Ortegal complex form a long band (15 × 0.1–2 km) bounded by thrust surfaces (Fig. 1). Most of the band is composed of eclogites with N-MORB composition, with kyanite and zoisite as accessories. Mg- and Al-rich eclogites with abundant kyanite, zoisite, and amphibole occur in several places within this band; the latter eclogites sometimes contain Cr-rich omphacite with patchy green pleochroism (up to 4 wt% Cr_2O_3, Gil Ibarguchi et al., 1990). In the course of this study, yellow to colorless staurolite with X_{Mg} ca. 0.31–0.35 (see below, samples 38 and 400) associated with amphibole and corundum, has been found in these eclogites as armored relics within garnet. The kyanite-staurolite-bearing rocks form elongated lenses (up to 10 × 1 m) within the common (N-MORB) eclogites. They have been found in situ only at one place 200 m above the lighthouse near the Cabo Ortegal Point. They occur as loose blocks in the hillside below the outcrop and as debris produced during construction of the road to the lighthouse. In hand sample, the kyanite-staurolite-bearing rocks are medium to coarse grained with pink centimeter-size garnets in a bright green matrix, locally veined with white zoisite and blue kyanite concentrations.

The kyanite-staurolite-bearing rocks show granonematoblastic texture with foliation and mineral lineation, defined by elongate crystals of amphibole, zoisite, and kyanite, parallel to corresponding structures in enclosing eclogites (elongated omphacite). The rocks are composed, in decreasing order of abundance, of hornblende, garnet, zoisite, kyanite, staurolite, and spinel as primary phases. An extensive search for pyroxene, a common phase in associated eclogites, was unsuccessful.

Amphibole occurs as large (up to 1 cm), elongate porphyroblasts containing rare inclusions of rounded, aligned, colorless kyanite and exceedingly rare tiny prisms of zoisite. Amphibole is mostly subidiomorphic, although anhedral porphyroblasts embaying garnet are not uncommon (Fig. 2). It is generally colorless, with some crystals presenting a feeble light-green pleochroism. Garnet forms subidiomorphic, 0.5–1 cm crystals commonly rich in minute inclusions of zoisite ± amphibole dispersed in patches that give a strongly sieved appearance to this mineral (Fig. 2). Zoisite occurs either as colorless, 0.5–4 mm, prismatic crystals forming oriented aggregates in the matrix, or as smaller grains (<1 mm) randomly oriented forming patchy inclusions in garnets (Fig. 2).

Kyanite occurs as 0.1–3 mm, tabular grains, often

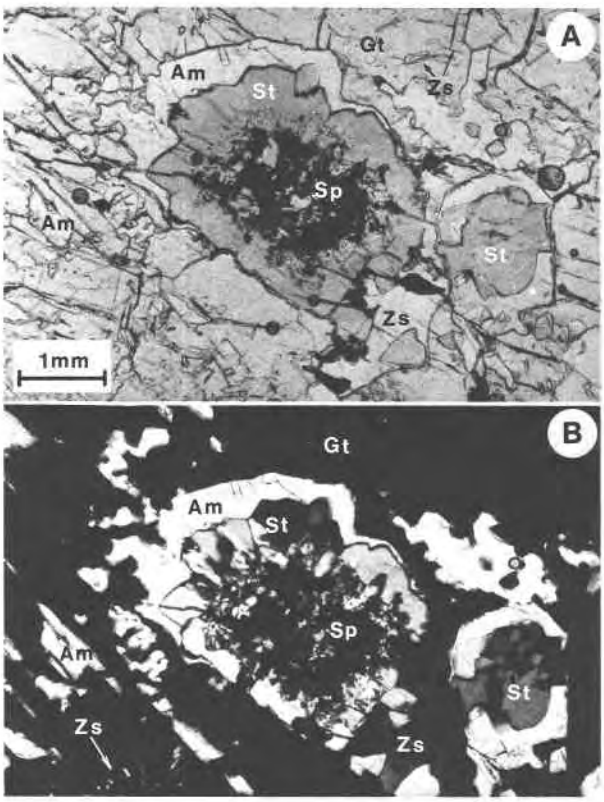

Fig. 2. Photomicrographs of the kyanite-staurolite-bearing rock. (**A**) Plane-polarized light. (**B**) Crossed polars. Abbreviations are as follows: St = Mg- and Cr-rich staurolite with penetration twins, Gt = garnet, Sp = spinel, Am = amphibole, Zs = zoisite.

Table 1. Chemical composition of kyanite-staurolite rock and associated eclogite

Sample	CO 80	CO 97		CO 80	CO 97
SiO_2	44.21	48.20	Ba	8	<5
Al_2O_3	21.53	15.08	Be	<0.5	0.6
Fe_2O_3	5.08*	12.16*	Co	61	156
MnO	0.07	0.17	Cr	898	271
MgO	13.83	8.30	Cu	133	42
CaO	12.44	12.17	Nb	<5	<5
Na_2O	0.96	2.17	Ni	370	87
K_2O	0.40	—	Rb	13	5
TiO_2	0.07	1.31	Sc	13.19	51.2
P_2O_5	0.11	0.19	Sr	106	73
I.L.	1.76	0.08	Th	<5	<5
Total	100.46	99.83	V	16	332
			Y	<5	32
Niggli norm**:			Zn	36	57
			Zr	7	66
Or	2.27	—			
Ab	5.89	18.61	La	0.63	2.78
An	51.09	30.00	Nd	0.73	7.36
Ne	1.43	—	Eu	0.16	0.87
En	—	1.36	Dy	0.38	4.96
Fs	—	1.33	Yb	0.28	3.05
Ol	31.50	22.60	Ce	8.32	16.00
Di	5.93	21.18	Sm	0.75	3.13
Mt	1.57	2.81	Gd	0.58	3.68
Ilm	0.09	1.74	Er	0.32	3.11
Ap	0.22	0.38	Lu	0.06	0.59

Note: 80 = kyanite-staurolite rock; 97 = associated eclogite; major elements in wt%; trace elements in ppm.
* All Fe as Fe_2O_3.
** Fe^{3+}/Fe^{2+} correction according to Irvine and Baraggar (1971).

twinned, forming elongate, oriented aggregates in the matrix. Locally, kyanite occurs as small, colorless crystals included in amphibole. Matrix kyanite often exhibits a patchy pleochroism (X = pale blue, Y = Z = colorless to pale yellow). Small inclusions of Cr-rich spinel are occasionally found within matrix kyanite. Staurolite forms subidiomorphic, 0.1–5 mm crystals, appearing in contact with garnet, amphibole, kyanite, and, more rarely, with zoisite (Fig. 2). Most staurolites exhibit penetration twins (Fig. 2) and patchy, light green–light yellow pleochroism; less abundant are yellow to colorless staurolites, which may occur with the green ones in the same thin section. Spinel occurs as brown, interstitial grains in blue kyanite (± staurolite) aggregates or as armored relics within green staurolite (Fig. 2) and, more rarely, within kyanite. Subidiomorphic sulfides rich in Fe, Cu, and less Zn, are also present; in some cases, the sulfide surrounds a core of magnetite.

Retrogression is observed along thin, fine-grained zones subparallel to the main foliation. Secondary symplectitic zoisite after primary zoisite and kyanite, as well as Mg-rich chlorite, muscovite, and corundum, appear in these zones. Locally, small crystals of light green fibrous amphibole surrounds garnet and fills fractures of this mineral, and fibrous margarite surrounds sulfide crystals.

Bulk-rock chemistry

Major and trace elements, including rare earths (REE), were determined by X-ray fluorescence and inductively coupled plasma atomic emission spectrometry at the CRPG (Research Center for Geochemistry, Nancy, France; cf. Govindaraju and Mevelle, 1987 for analytical details) on one fresh sample of kyanite-staurolite-bearing rock and one associated eclogite. Bulk chemical analyses and norms are given in Table 1. Enrichments in Ce and Lu and depletion in Nd (Fig. 3) likely represent analytical artifacts since analogous eclogites analyzed by mass spectrometry at the University of Rennes (Bernard-Griffiths et al., 1985; Peucat et al., 1990) have distinctly lower Ce and Lu contents (Fig. 3).

The kyanite-staurolite-bearing rock has less than 45 wt% SiO_2 (Table 1) and is ultrabasic according to the widely used classification based on the weight percentage of SiO_2 (Willians et al., 1982). According to Irvine and Baraggar's (1971) classification, the protolith could correspond to a picritic basalt of the sodic series. The REE pattern for the kyanite-staurolite-bearing rock (sample 80) is compared in Figure 3 with that of the associated eclogite (sample 97). REE patterns for eclogites elsewhere within the same band are also shown in Figure 3 for comparison (data from Bernard-Griffiths et al., 1985; Peucat et al., 1990). The eclogite associated with the kyanite-

staurolite-bearing rock has a composition similar to that of the common eclogites of the band characterized by their N-MORB geochemical features (Table 1, Fig. 3). The kyanite-staurolite-bearing rock, although having distinctly lower absolute concentrations (Table 1), displays a REE pattern similar to those of the Mg- and Al-rich eclogites (Fig. 3) with abundant kyanite ± zoisite and locally staurolite and Cr-rich omphacite for whose protoliths a cumulative origin has been suggested (Gil Ibarguchi et al., 1990).

The low REE contents of the kyanite-staurolite-bearing rock point towards a protolith rich in mafic phases, while the richness in Al_2O_3 (21.53 wt%) and CaO (12.44 wt%) and the lack of positive Eu anomaly suggest crystallization of anorthite-rich plagioclase under relatively high f_{O_2} conditions. The kyanite-staurolite-bearing rock analyzed is also notably richer in Mg, Al, Cr, Ni, and Cu and poorer in Si, Fe, Na, Ti, Co, V, Sc, REE, and Y than the N-MORB eclogites (Table 1, Fig. 3). These facts and the presence of Cr-rich spinel in minor amounts suggest that the protoliths of the kyanite-staurolite-bearing rocks represent an extreme product of the process that originated the Mg- and Al-rich eclogites of the same unit. Hence, the kyanite-staurolite-bearing rocks must have a cumulative origin from a magma comparable to a recent MORB that is the protolith of associated common eclogites.

Cr-rich kyanite- and/or Mg-rich staurolite-bearing rocks showing comparable bulk chemical compositions to those studied here have been described elsewhere as metatroctolites (Demange, 1976; Nicollet, 1986) or recrystallized Mg-rich, undersaturated, spinel-bearing anorthosites (Sobolev et al., 1968). To a certain extent, both rock names may be equivalent or at least related. However, in this case, the anorthositic hypothesis seems to be excluded in view of the REE pattern of the kyanite-staurolite-bearing rock (Fig. 3). An origin from a cumulate, spinel-bearing, plagioclase-rich peridotite to troctolite-picrite seems more likely.

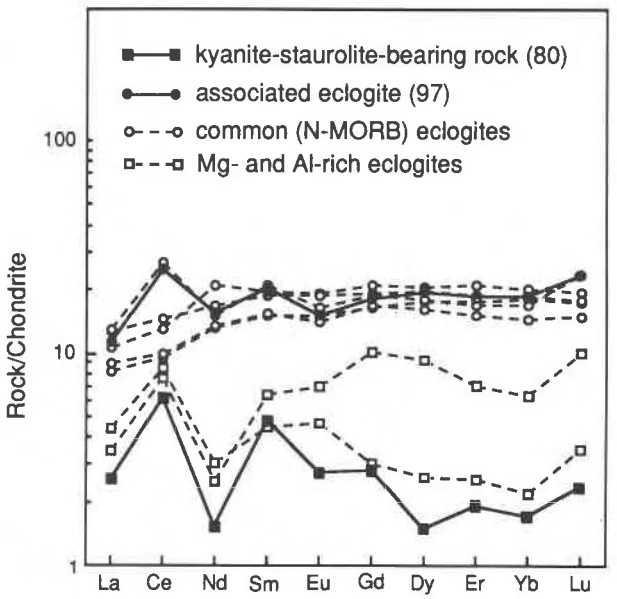

Fig. 3. Chondrite normalized REE distribution for various rock types within the eclogitic band at the Cabo Ortegal complex: (1) the kyanite-staurolite-bearing rock (sample 80, Table 1), (2) the associated eclogite (sample 97, Table 1), (3) the common eclogites with N-MORB composition (data from Bernard-Griffiths et al., 1985; Peucat et al., 1990), and (4) the Mg- and Al-rich eclogites (data from Gil Ibarguchi et al., 1990). Normalization values after Evensen et al. (1978).

Mineral chemistry

Minerals were analyzed at the universities of Clermont-Ferrand and Paris VI (France), and Oviedo (Spain) with Camebax Microbeam and SX50 automated microprobes equipped with three (Clermont and Oviedo) and four spectrometers (Paris), respectively. Operating parameters included a 10 s integration time, a ca. 10 nA beam current, and a 15 kV accelerating voltage. Calibration was against BRGM (French Geological Survey) standard minerals, and the ZAF correction procedure was used. The analytical error has been shown to be less than ca. 2% for most major elements for the microprobe at Clermont (Boivin, 1982). Tables 2–4 present a selection of minerals analyzed; the complete set of data used in this report is available from the first author on request. Mineralogical features are described below in order of decreasing abundance of mineral phases.

Amphibole

The overall composition of amphibole is Mg-rich (X_{Mg} > 0.9) tschermakitic hornblende to magnesiohornblende (Table 2). Some grains are slightly zoned with Fe^{3+}/Fe^{2+} ratios increasing from core to rim, however, no systematic zoning has been detected.

Garnet

Analyzed garnets are rich in pyrope, almandine, and grossular end-members. While Ca content remains relatively constant, Mg and Fe contents vary considerably among garnets from different samples. The maximum Mg content is usually recorded at the rims (Fig. 4), and X_{Mg} values may range from 0.62 (core) to 0.74 (rim) for a single garnet grain (Table 2); however, systematic zoning has not been detected. These garnets are richer in Mg, poorer in Fe, and somewhat poorer in Ca than those of the associated common eclogites (eclogites with N-MORB composition) or than those of the Mg- and Al-rich eclogites of the same area (Fig. 4).

Zoisite

Zoisite grains in the matrix and included in garnet have similar compositions with relatively low Fe_2O_3 contents (Table 2). X_{Fe} [= $Fe^{3+}/(Fe^{3+} + Al)$] values are ≤0.28; therefore, they cannot be considered ferrian zoisites (cf. Maaskant, 1985).

TABLE 2. Representative chemical analyses of amphibole, garnet, zoisite, and spinel

Sample	80 (am)	81 (gt, c)	81 (gt, r)	80 (zs)	80 (sp1)	80 (sp2)	80 (sp3)
SiO_2	49.39	39.41	40.9	39.5	bd	bd	0.04
TiO_2	0.11	0.03	0.02	0.06	0.05	0.01	bd
Al_2O_3	11.32	22.95	24.14	32.34	16.61	38.42	21.11
Cr_2O_3	0.05	0.18	0.06	0.23	50.74	28.67	45.93
FeO_t	3.02	15.03	10.83	1.18	25.56	19.99	24.5
MnO	bd	0.61	0.14	0.16	0.22	0.07	0.11
NiO	na	0.09	bd	0.09	0.02	bd	bd
ZnO	na	na	na	na	na	na	0.89
MgO	18.35	13.19	17.51	0.09	6.21	11.57	6.99
CaO	12.51	7.85	6.31	24.53	bd	bd	bd
Na_2O	1.20	0.03	0.02	bd	bd	bd	0.02
K_2O	0.17	0.03	bd	0.01	bd	bd	bd
Total	96.12	99.4	99.93	98.18	99.41	98.73	99.59
Si	6.924	2.92	2.935	6.003	bd	bd	0.1
Al	1.871	2.005	2.042	5.794	0.65	1.332	0.81
Ti	0.012	0.002	0.001	0.006	0.001	<0.001	bd
Cr	0.006	0.01	0.003	0.027	1.329	0.667	1.118
Fe^{3+}	0.137	0.063	0.018	0.135	0.02	0.001	0.009
Fe^{2+}	0.217	0.869	0.632		0.688	0.491	0.657
Mn	bd	0.038	0.008	0.02	0.006	0.002	0.003
Mg	3.834	1.457	1.872	0.021	0.307	0.507	0.339
Ni	na	0.005	bd	0.011	0.001	bd	bd
Zn	na	na	na	na	na	na	0.021
Ca	1.879	0.623	0.485	3.993	bd	bd	bd
Na	0.326	0.004	0.003	0.001	bd	bd	0.001
K	0.03	0.003	bd	0.002	bd	bd	bd

Note: 80, 81 = kyanite-staurolite rocks; am = amphibole (normalization by summing cations exclusive of K + Ca + Na to 13 and Fe^{3+} evaluated by charge balance considerations); gt = garnet (c = core, r = rim, normalization to total cations = 8, Fe^{3+} = 2-$Al^{(6)}$-Ti-Cr); zs = zoisite (all Fe as Fe^{3+}, 25 O atoms in formula); sp = spinel (1 = armored relic in staurolite, 2 = interstitial light-brown, 3 = interstitial dark-brown, Fe^{3+} determined by charge balance calculations on the basis of 4 O atoms and 3 cations); bd = below detection limit of 0.01 wt%; na = not analyzed.

Kyanite

Representative analyses of colored and colorless kyanite are presented in Table 3. Blue color in kyanite has been correlated with Fe^{3+}, Fe^{2+}, and Ti concentrations (Smith and Strens, 1976; Parkin et al., 1977; cf. Cooper, 1980 for other references). Colorless kyanites are distinctly poorer in Cr (Table 3, Fig. 5A), but Fe and Ti do not vary appreciably. The kyanite is not zoned, although Cr contents may vary considerably within a single grain (cf. standard deviations in Table 3). Ti and Fe contents are normal for this mineral, but the Cr contents, with a maximum of 4.35 wt% Cr_2O_3, are unusual. Kyanite richer in Cr has been reported only by Sobolev et al. (1968) from grospydite xenoliths in the kimberlites of Yakutia (12.86 wt% Cr_2O_3). Cooper (1980) has reported kyanite with 1.44 wt% Cr_2O_3 in amphibolites from South Westland (New Zealand), and with up to 2.88 wt% Cr_2O_3 in metacherts from the same area. Variations in Cr and Al concentration seem to be independent of Fe content in kyanite, which is always low (Table 3). Good correlation between Cr and Al content, as shown in Figure 5A, suggests that Cr substitutes for Al in the kyanite structure. There is, however, a significant difference between observed and ideal Al = Cr substitution. (Adding Fe to Cr does not significantly modify the result because of the low amounts of Fe in kyanite.)

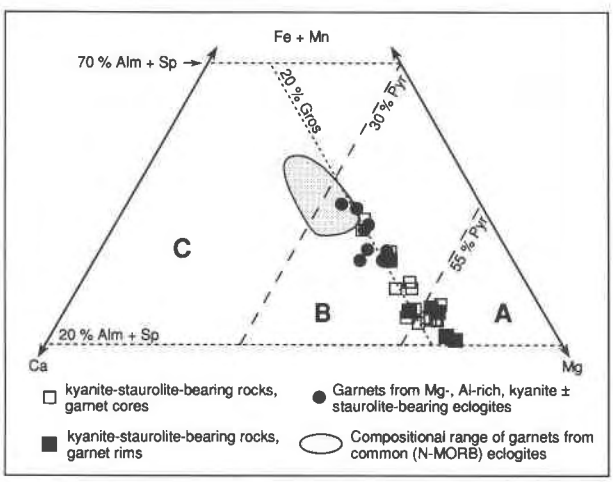

Fig. 4. Composition of garnet (mol%). Squares = garnets from the kyanite-staurolite-bearing rocks (open squares = cores, solid squares = rims). Solid circles = garnets from Mg- and Al-rich eclogites. Shaded area = compositional range of garnets from common (N-MORB) eclogites. Fields for eclogites of types A, B, and C after Coleman et al. (1965).

The miscibility of Cr in kyanite has been experimentally investigated by Seifert and Langer (1970) who found that more Cr-rich kyanite is stabilized by higher pressures. This suggests that kyanite formed in these rocks during increasingly higher pressure conditions because the earliest kyanite is the Cr-poor, colorless crystals included in amphibole, whereas blue kyanite, formed later in the matrix, exhibits considerably higher Cr content. In contrast to the experiments, however, the rocks with kyanite and staurolite are not saturated with Cr and thus variations in Cr content could be dependent on the availability

TABLE 3. Chemical analyses of kyanite

Sample	80 (ky, bl) $n = 5$	std. dev.	80 (Cr_{max})	81 (ky, bl) $n = 4$	std. dev.	81 (ky, col)
SiO_2	36.52	0.28	36.94	36.61	0.57	36.92
TiO_2	0.01	0.01	bd	0.03	0.02	bd
Al_2O_3	58.39	0.59	58.89	61.1	0.42	63.15
Cr_2O_3	3.85	0.46	4.35	2.44	0.28	0.26
FeO_t	0.21	0.04	0.17	0.27	0.09	0.26
MnO	0.04	0.03	0.06	0.01	0.02	bd
NiO	0.01	0.02	bd	bd		bd
MgO	0.02	0.01	0.03	0.02	0.01	0.02
CaO	bd		bd	0.02	0.02	0.02
Na_2O	0.03	0.05	0.12	bd		0.01
K_2O	0.02	0.02	0.04	0.01	0.01	0.01
Total	99.14		100.62	100.55		100.68
Si	1.007		1.006	0.992		0.991
Al	1.899		1.89	1.951		1.999
Ti	<0.001		bd	0.001		bd
Cr	0.084		0.094	0.052		0.006
Fe^{3+}	0.08		0.004	0.005		0.006
Mn	0.001		0.001	<0.001		bd
Mg	<0.001		0.001	0.001		0.001
Ni	<0.001		bd	bd		bd
Ca	bd		bd	0.001		0.001
Na	0.001		0.006	bd		0.001
K	0.001		0.001	<0.001		<0.001

Note: 80, 81 = kyanite-staurolite rocks; ky = kyanite (bl = blue, col = colorless, Cr_{max} = analyzed kyanite with maximum content in Cr); all Fe considered as Fe^{3+} in the structural formulae; bd = below detection limit of 0.01 wt%; n = number of analyses in the same crystal; std. dev. = standard deviation.

of Cr in the rock. The presence, locally, of small inclusions of Cr-rich spinel within blue kyanite in the matrix suggests that Cr contents in kyanite and associated spinel may be related by a reaction such as Al_2SiO_5 (in kyanite) + $FeCr_2O_4$ (in spinel) = Cr_2SiO_5 (in kyanite) + $FeAl_2O_4$ (in spinel). Because it has not been determined whether increasing pressure drives this reaction to the right, Seifert and Langer's (1970) results must be applied with caution to these rocks.

Staurolite

Representative analyses of green and yellow staurolite are presented in Table 4; chemical formulae were calculated on the basis of Si + Al + Cr = 25.53, as recommended by Holdaway et al. (1986). It may be observed from the data in Table 4 and those plotted in Figures 5B and 6 that the green staurolite is distinctly richer in Cr than the yellow staurolite. X_{Mg} values of both types of staurolite are higher than those of the staurolite in the Mg- and Al-rich eclogites (samples 38 and 400, Table 4, Fig. 6). The staurolite grains in the kyanite-staurolite-bearing rocks exhibit considerable heterogeneity. X_{Mg} ranges from 0.579 to 0.726 (average) for different crystals of green staurolite in one sample (82). The variations are even greater considering different types of staurolite; Cr_2O_3 ranges from 6.26 wt% for green staurolite to 0.27 in yellow staurolite grains in sample 80. In a few cases, Cr values may also differ considerably within the same crystal (e.g., 0.33 to 2.03 wt% Cr_2O_3 in one crystal from sample 81). Ti, Ni, Mn, and Zn concentrations are low in analyzed staurolite.

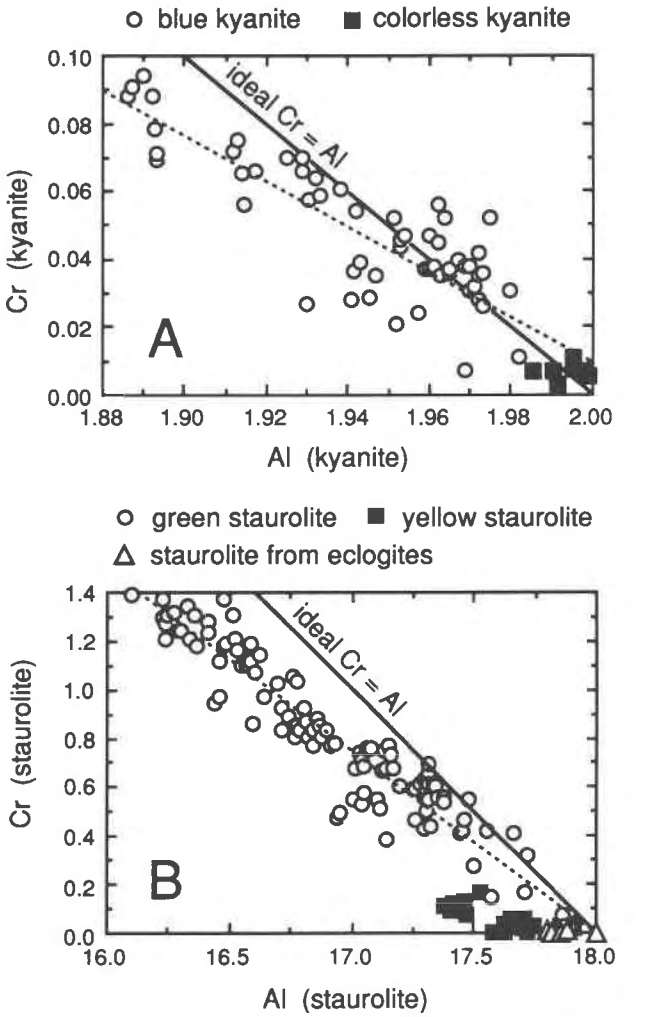

Fig. 5. (**A**) Cr vs. Al for kyanite from kyanite-staurolite-bearing rocks; the least squares regression line shown for blue kyanite is $y = 1.233 - 0.6093x$ ($r = 0.84$). (**B**) Cr vs. Al for staurolite from kyanite-staurolite-bearing rocks (green and yellow staurolite) and from Mg- and Al-rich eclogites (open triangles). The least squares regression line shown for green staurolite is $y = 13.1359 - 0.7286x$ ($r = 0.95$).

The magnesian (up to 0.744 X_{Mg}) and chromian (up to 6.43 wt% Cr_2O_3) compositions of the staurolite (Table 4) are unusual. Staurolite with higher X_{Mg} ratio has been found only as rare inclusions within pyrope crystals in metasediments at the Dora Maira massif, western Alps (Chopin, 1987; $X_{Mg} = 0.80$–0.95), while comparable high-X_{Mg} values ($X_{Mg} = 0.737$ as average) have been reported from staurolite occurring as pseudomorphs after garnet, corundum, and kyanite within ultramafics from Donghai District, China (Enami and Zang, 1988). The maximum Cr content so far recorded was 2.2 wt% Cr_2O_3 in metatroctolites from Madagascar (Nicollet, 1986), which is much lower than the values for staurolite analyzed in this study.

Ward (1984) has reported a Cr_2O_3 content of 2.01 wt%

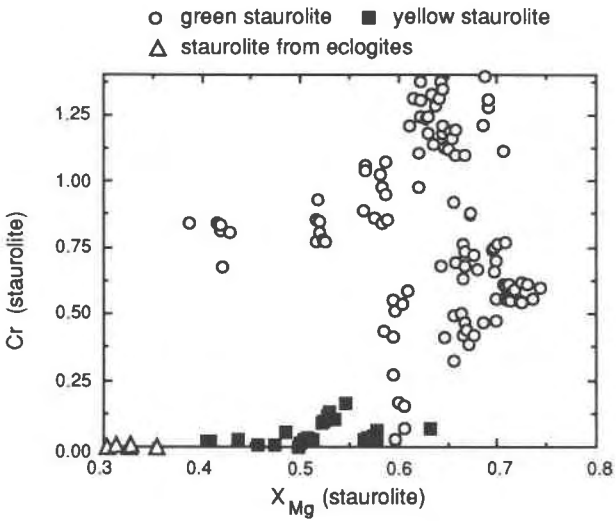

Fig. 6. Cr vs. X_{Mg} [= Mg/(Mg + Fe)] for staurolite from kyanite-staurolite-bearing rocks (green and yellow staurolite) and from Mg- and Al-rich eclogites (open triangles).

in a staurolite; he pointed out that the absence of a chromite phase implied that the recorded values need not represent saturated Cr contents. [Actually, reported atomic Cr/(Cr + Al) is lower than in coexisting, Cr-poor minerals.] Nicollet (1986) has reported a Cr_2O_3 content of 2.2 wt% in staurolite coexisting with moderately Cr-rich spinel (8.3 wt% Cr_2O_3). In the present case, analyzed staurolite presents higher Cr/(Cr + Al) ratios than relatively Cr-rich coexisting minerals (0.08, vs. 0.047 in Cr-rich kyanite), which may indicate partitioning of Cr into staurolite. In addition, analyzed staurolite shows higher Cr contents when it contains inclusions of chromite (e.g., one staurolite in sample 80 with 5.81 wt% Cr_2O_3 as average, contains chromite with as much as 50.74 wt% Cr_2O_3, Tables 2 and 4), which suggests that the recorded values may represent near-saturation Cr contents. It may be noted that Cr contents in staurolite do not correlate with X_{Mg} values in the same mineral (Fig. 6), which is consistent with previous findings of high Cr contents both in Mg- and Fe-rich staurolite (Demange, 1976; Ward, 1984; Nicollet, 1986).

Average Si contents per formula unit range from ca. 7.5 to 8. These values are comparable to those reported from most magnesian staurolite samples in the literature (e.g., Schreyer et al., 1984; Ward, 1984; Nicollet, 1986; Enami and Zang, 1988; using the Si + Al + Cr = 25.53 normalization scheme for formula calculation).

Substitutions of Al by Cr and of 3(Mg,Fe) = 2Al in octahedral sites are indicated by good negative correlations between Al vs. Cr and (Fe + Mg + Mn + Zn) vs. Al′ + Ti + Cr, where Al′ = Al + Si − 8, (Figs. 5B and 7). As in the case of kyanite, there is, however, a significant difference between observed and ideal Al = Cr substitution (Fig. 5B). Staurolite closely follows the maximum likelihood line calculated by Griffen et al. (1982), or that of Grew and Sandiford (1985), when Ti, as suggested by Schreyer et al. (1984), and Cr are added to Al′ (Fig. 7B). Otherwise, only the yellow staurolite approaches the trend corresponding to the second substitution,

TABLE 4. Chemical analyses of staurolite

Sample	80 (st, gt) $n = 5$	std. dev.	80 (Cr_{max})	80 (st, yel) $n = 5$	std. dev.	81 (mg_{max})	38	400
SiO_2	29.23	0.24	29.3	28.92	0.14	29.03	27.63	27.71
TiO_2	0.20	0.08	0.24	0.14	0.1	0.14	0.16	0.15
Al_2O_3	50.28	0.71	49.77	53.76	0.51	55.27	54.02	55.03
Cr_2O_3	5.81	0.46	6.43	0.55	0.16	2.85	0.03	0.02
FeO_t	5.44	0.14	5.59	8.88	0.19	4.13	12.58	12.14
MnO	0.05	0.04	0.05	0.13	0.05	bd	0.08	0.12
NiO	0.03	0.04	0.09	0.03	0.01	0.11	bd	0.03
ZnO	bd		bd	0.1	0.07	0.24	bd	0.2
MgO	6.88	0.09	6.92	5.69	0.12	6.72	3.21	3.33
CaO	0.07	0.05	0.07	0.09	0.08	bd	bd	0.02
Na_2O	bd		bd	bd		0.01	bd	0.01
K_2O	0.02	0.03	bd	0.07	0.05	0.01	bd	bd
Total	98.01		98.44	98.36		98.49	97.71	98.74
Si	8.015		8.038	7.96		7.685	7.723	7.64
Al	16.256		16.1	17.449		17.248	17.8	17.88
Ti	0.042		0.05	0.029		0.027	0.034	0.031
Cr	1.259		1.394	0.12		0.597	0.007	0.005
Fe	1.247		1.282	2.044		0.914	2.941	2.798
Mn	0.012		0.01	0.03		bd	0.019	0.028
Mg	2.813		2.829	2.336		2.649	1.337	1.368
Ni	0.007		0.019	0.007		0.023	bd	0.006
Zn	bd		bd	0.021		0.046	bd	0.004
Ca	0.019		0.021	0.027		bd	bd	0.004
Na	bd		bd	bd		0.005	bd	0.003
K	0.006		bd	0.025		0.002	bd	bd

Note: 80, 81 = kyanite-staurolite rocks; 38, 400 = eclogites with yellow staurolite; st = staurolite (gr = green, yel = yellow); Cr_{max} = analyzed staurolite with maximum content in Cr, mg_{max} = analyzed staurolite with maximum mg ratio [mg = Mg/(Mg + Fe)]; bd = below detection limit of 0.01 wt%; n = number of analyses in the same crystal; std. dev. = standard deviation.

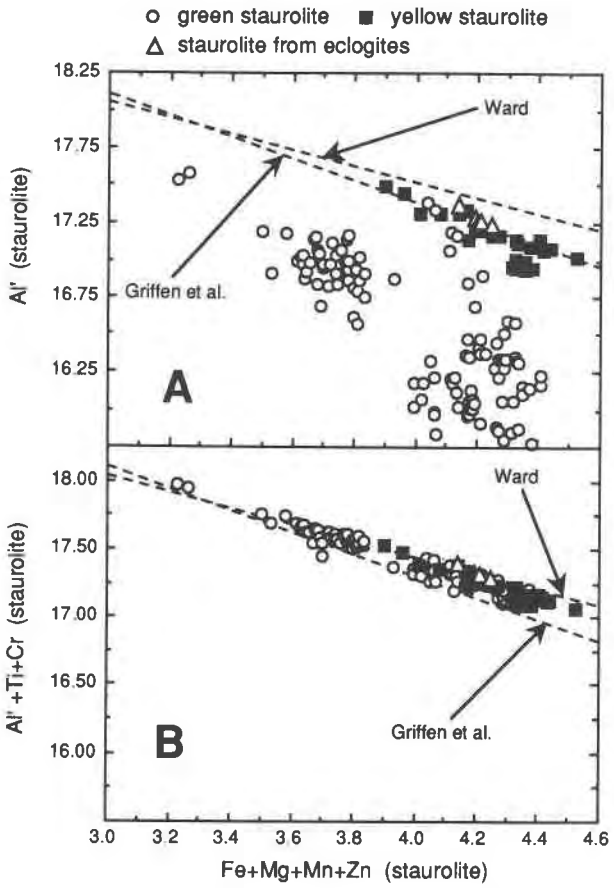

Fig. 7. (Fe + Mg + Mn + Zn) vs. Al′ (**A**) and vs. (Al′ + Ti + Cr) (**B**), for staurolite from kyanite-staurolite-bearing rocks (green and yellow staurolite) and from Mg- and Al-rich eclogites (open triangles). Al′ = Al + Si − 8. The maximum likelihood lines of Griffen et al. (1982) and Ward (1984, calculated by Grew and Sandiford, 1985) are shown. A least squares regression line (not shown) for analyzed staurolite from the kyanite-staurolite-bearing rocks corresponds to $y = 20.2031 - 0.7017x$ ($r = 0.98$). (Not having the data to renormalize analyses from the literature, we have used the same normalization as the authors cited, i.e., cationic proportions are here on the basis of 46 O atoms.)

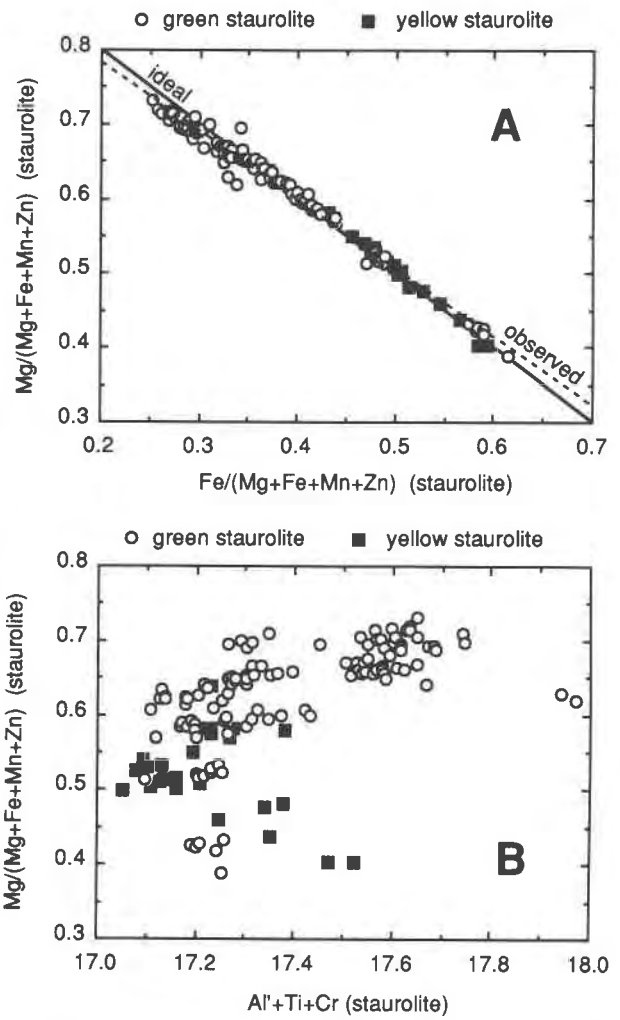

Fig. 8. Mg/(Mg + Fe + Mn + Zn) vs. Fe/(Mg + Fe + Mn + Zn) (**A**) and vs. Al′ + Ti + Cr (**B**), for green and yellow staurolite from kyanite-staurolite-bearing rocks. The least squares regression line for all staurolite plotted in **A** corresponds to $y = 0.967 - 0.9206x$ ($r = 0.985$).

whereas the green staurolite plots far below that trend (Fig. 7A).

Mg incorporation seems to be accounted for by a Mg = Fe substitution scheme, as deduced from the plot of Mg/(Mg + Fe + Mn + Zn) vs. Fe/(Mg + Fe + Mn + Zn) [Fig. 8A; this is an Mg vs. Fe plot in which variation of (Fe + Mg + Mn + Zn) vs. Al′ is canceled]. In contrast, there is no correlation between Mg content or X_{Mg} values and other cation contents, such as cation total or cations in staurolite monolayer except for Al′ (i.e., FM = Fe + Mn + Mg + Zn + Co + Ni + Li + Ti) as suggested by Ward (1984) and Enami and Zang (1988) for Mg-rich staurolite elsewhere. Neither is Mg incorporation controlled by an $^{[6]}$Al = Mg + H substitution scheme as deduced from the lack of correlation between Al′ + Ti + Cr and Mg/(Mg + Fe + Mn + Zn) (Fig. 8B). Staurolite is characteristically lower in X_{Mg} than coexisting silicates, although X_{Mg} staurolite > X_{Mg} garnet is common in many low- to medium-pressure metapelites (Ballèvre et al., 1989 and references therein). Reversals in Fe-Mg partitioning have also been experimentally obtained by Rice (1985) and proposed on the basis of staurolite solution models by Holdaway et al. (1988). In this case, the maximum X_{Mg} values recorded are, within the limits of analytical error, similar for both staurolite and garnet: 0.744 and 0.748, respectively. Compared with coexisting amphibole, however, staurolite has consistently lower X_{Mg} values (>0.9 in amphibole).

Spinel

Representative analyses of interstitial grains of spinel in blue kyanite (± staurolite) aggregates and of armored

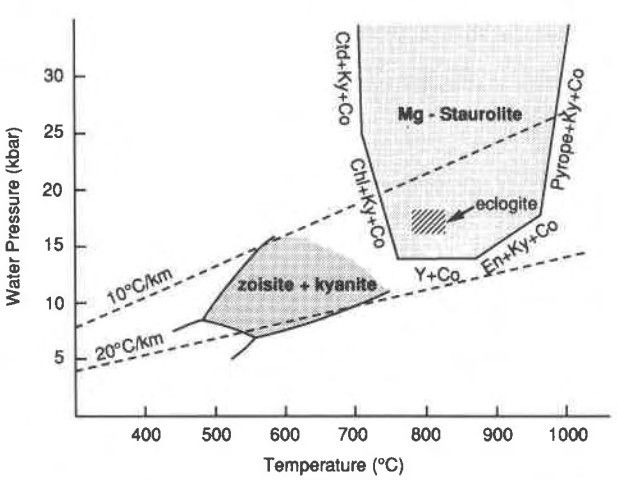

Fig. 9. Approximate stability fields (stippled areas) of zoisite + kyanite (after Chatterjee, 1976) and magnesium staurolite (after Schreyer, 1988) relative to linear geotherms. The area labeled eclogite corresponds to the pressure and temperature estimate for the eclogite enclosing the kyanite-staurolite-bearing rocks (after Gil Ibarguchi et al., 1990). Abbreviations are as follows: Ctd = magnesium chloritoid, Ky = kyanite, Co = corundum, Chl = chlorite, Y = yoderite, En = enstatite.

relics within green staurolite are presented in Table 2. Interstitial grains show highly variable composition. Most of them correspond to Cr-rich spinel with rather variable Cr/Al ratios, even within a single crystal, but Fe^{2+}-rich chromite may be present too. Dark brown crystals are richer in Cr than light brown ones. Crystals enclosed in green staurolite correspond to Fe^{2+}-rich chromite, similar in composition to the interstitial grains, although richer in Cr.

Petrogenetic interpretation

The observed association of hornblende-garnet-zoisite-kyanite-staurolite may be considered as one of the several subassemblages that may develop from the chemical system SiO_2-Al_2O_3-Fe_2O_3-TiO_2-FeO-MgO-MnO-CaO-K_2O-Na_2O-H_2O-CO_2. Selverstone et al. (1984) presented a graphical analysis of the assemblages for two 12-phase suites within this system, including the five phases mentioned. According to these authors, the unusual mineral association of hornblende + kyanite + staurolite is indicative of reactions such as plagioclase + chlorite + epidote = hornblende + staurolite + kyanite + paragonite, which must take place under conditions "not commonly attained during regional metamorphism." A reaction grid for K-poor pelitic and mafic rocks presented by Froese and Hall (1983) suggests that these are high pressure and temperature conditions.

Textural data indicate that zoisite and colorless kyanite were the first metamorphic phases to form in the rocks; staurolite, garnet, blue kyanite, and amphibole, along with more zoisite and colorless kyanite, formed later. Textural and mineralogical evidence suggest that blue kyanite and green staurolite formed through reactions involving destruction of Cr-rich spinel. The latter mineral, having the greatest affinity for Cr [Cr/(Cr + Al) up to 0.67 vs. 0.08 in staurolite and 0.05 in kyanite], should become progressively enriched in Cr, which explains the presence of armored relics of chromite and of spinel grains with variable Cr/Al ratios. The remaining kyanite, zoisite, garnet, staurolite, and amphibole should form through recrystallization of primitive igneous phases or of their lower-grade metamorphic equivalent. The latter could likely be plagioclase, chlorite, and epidote as suggested above; however, except for the occurrence of zoisite inclusions within garnet and, more rarely, within amphibole, and of some kyanite inclusions within the latter mineral, there is no textural evidence of reactions involved.

Minimum *P-T* conditions for the first metamorphic association recorded, i.e., colorless kyanite + zoisite included in other minerals, may be inferred from experimental results by Chatterjee (1976) for this assemblage: 450–550 °C and 6–8 kbar, assuming $a_{H_2O} = 1$ (Fig. 9, values reach 600 °C, 9 kbar if results by Newton, 1966 and Storre and Nitsch, 1974 are considered). Subsequent evolution should be toward higher *P* and *T*, since Cr-rich kyanite and Mg-rich staurolite that formed later are known from experiment to be stable under high pressure and temperature conditions (Schreyer, 1968; Schreyer and Seifert, 1969; Seifert and Langer, 1970; Hellman and Green, 1979). Using the experimental data obtained by Schreyer (1968) and Schreyer and Seifert (1969), Schreyer (1988) showed that the stability field of magnesium staurolite covers a wide range from approximately 13 to far greater than 50 kbar and from 700 to greater than 1000 °C (Fig. 9). Hellman and Green (1979) reported synthesis of Mg-rich staurolite ($X_{Mg} > 0.52$), from an olivine tholeiite of composition not very different from that of the rocks studied here, at pressures of 24–26 kbar and temperatures of 740–760 °C. It may be noted that *P-T* conditions calculated for associated eclogites, ca. 800 °C, >17 kbar, (Fig. 9, Gil Ibarguchi et al., 1990) are in the range of *P-T* values that may be assumed for the formation of Mg-rich staurolite and Cr-rich kyanite. These *P-T* values are consistent with the structural evidence that the hornblende-garnet-zoisite-kyanite-staurolite-bearing rocks have undergone the same deformation events as enclosing eclogites.

An attempt to estimate *T* conditions during the eclogitic episode in the hornblende-garnet-zoisite-kyanite-staurolite rocks using available calibrations for garnet-staurolite and garnet-hornblende equilibria (Perchuk, 1977; Perchuk et al., 1985; Powell, 1985) yield scattered results. This is quite likely caused by the high Ca content in garnet, the low Fe concentration in amphibole, and the variable Fe-Mg ratio of staurolite. Staurolite and garnet in mutual contact from sample 81 yield a temperature of ca. 700 °C, but use of mineral compositions of garnet and staurolite not in contact from the same thin section results in temperatures from 685 to 870 °C. Calibrations of garnet-hornblende equilibrium by Perchuk et al. (1985)

and Powell (1985) yield comparable, very scattered results: 550–740 and 515–715 °C, respectively.

Conclusions

Mg- and Cr-rich staurolite [up to 0.744 Mg/(Mg + Fe) and 6.43 wt% Cr_2O_3] and Cr-rich kyanite (up to 4.35 wt% Cr_2O_3) occur in metamorphosed, Al-rich, ultrabasic rocks associated with eclogites in the Cabo Ortegal complex. Green pleochroism of staurolite and blue pleochroism of kyanite presumably result from Cr substitution for Al in octahedral sites of these minerals. Mg incorporation in staurolite requires cation substitution in tetrahedral Fe sites.

The formation of an earlier Cr-poor kyanite + zoisite assemblage in the rocks studied suggests a former metamorphic stage under *P-T* conditions greater than 450–550 °C and 6–8 kbar. Mg- and Cr-rich staurolite and Cr-rich kyanite formed subsequently in these rocks through reactions involving destruction of, and Cr enrichment in, Cr-rich spinel. These reactions likely took place during the eclogitic episode, for which *P-T* conditions have been estimated at ca. 800 °C, >17 kbar. It appears that under these conditions staurolite has a greater affinity for Cr relative to Al than coexisting kyanite. It is also observed that, in spite of considerable variations, Mg/Fe ratios in staurolite are consistently lower than those in the coexisting amphibole, but as high as those of the associated garnet.

We suggest that Mg- and Cr-rich staurolite and Cr-rich kyanite were stable through eclogitic metamorphism. High Mg contents in staurolite may be good indicators of elevated pressures during metamorphism of hydrous basic/ultrabasic compositions. Although the Cr contents of kyanite and staurolite could indicate Cr-rich bulk composition, the occurrence of small, colorless, Cr-poor kyanite included in matrix minerals and blue, Cr-rich, matrix kyanite suggest increasing Cr substitution in kyanite with increasing pressure and temperature. Mg-rich calcic amphibole, instead of pyroxene, was apparently a stable phase during eclogitic metamorphism in the kyanite-staurolite-bearing rocks, but evaluation of equilibrium conditions on the basis of published garnet-staurolite and garnet-hornblende calibrations points to the need for further experimental and thermodynamic modeling than that presently available.

Acknowledgments

We would like to thank E.-an Zen and Edward S. Grew for their constructive criticism. Finanical support by UPV and DGICYT grants (130/310-139.89 and PB89-0411) to J.I.G.I. and M.M., and by French-Spanish Cooperation Project (112) to J.I.GI., M.M., and J.G. is acknowledged.

References cited

Arenas, R., Gil Ibarguchi, J.I., Gonzalez Lodeiro, F., Klein, E., Martinez Catalán, J.R., Ortega Girones, E., de Pablo Maciá, J.G., and Peinado, M. (1986) Tectonostratigraphic units in the complexes with mafic and related rocks of the NW of the Iberian Massif. Hercynica, II, 2, 87–110.

Ballèvre, M., Pinardon, J.L., Kienast, J.R., and Vuichard, J.P. (1989) Reversal of Fe-Mg partitioning between garnet and staurolite in eclogite-facies metapelites from the Champtoceux Nappe (Brittany, France). Journal of Petrology, 30, 1321–1349.

Bernard-Griffiths, J., Peucat, J.J., Cornichet, J., Iglesias Ponce de Leon, M., and Gil Ibarguchi, J.I. (1985) U-Pb, Nd isotope and REE geochemistry in eclogites from the Cabo Ortegal Complex, Galicia, Spain: An example of REE immobility conserving MORB-like patterns during high-grade metamorphism. Chemical Geology (Isotope Geoscience Section), 52, 217–225.

Boivin, P. (1982) Interactions entre magmas basaltiques et Manteau Supérieur, 344 p. Thèse Université Clermont-Ferrand, Clermont-Ferrand, France.

Chatterjee, N.D. (1976) Margarite stability and compatibility relations in the system $CaO-Al_2O_3-SiO_2-H_2O$ as a pressure-temperature indicator. American Mineralogist, 61, 699–709.

Chopin, C. (1987) Very high-pressure metamorphism in the western Alps: Implications for subduction of continental crust. Philosophical Transactions of the Royal Society of London, ser. A, 321, 183–197.

Coleman, R.G., Lee, D.E., Beatty, L.B., and Brannock, W.W. (1965) Eclogites and eclogites: Their differences and similarities. Geological Society of America Bulletin, 76, 483–508.

Cooper, A.F. (1980) Retrograde alteration of chromian kyanite in metachert and amphibolite whiteschist from the Southern Alps, New Zealand, with implications for uplift on the Alpine Fault. Contributions to Mineralogy and Petrology, 75, 153–164.

Demange, M. (1976) Une paragenèse à staurotide et tschermakite d'Ovala (Gabon). Bulletin de la Société Française de Minéralogie et Cristallographie, 99, 379–402.

Enami, M., and Zang, Q. (1988) Magnesian staurolite in garnet-corundum rocks and eclogite from the Donghai district, Jiangsu province, east China. American Mineralogist, 73, 48–56.

Evensen, M.M., Hamilton, P.J., and O'Nions, R.K. (1978) Rare-earth abundances in chondritic meteorites. Geochimica et Cosmochimica Acta, 42, 1199–1212.

Froese, E., and Hall, R.D. (1983) A reaction grid for potassium-poor pelitic and mafic rocks. Current research, part A, Geological Survey of Canada, Paper 83-1A, 121–124.

Gil Ibarguchi, J.I., Mendia, M., Girardeau, J., and Peucat, J.J. (1990) Petrology of eclogites and clinopyroxene-garnet metabasites from the Cabo Ortegal complex (Northwestern Spain). Lithos, 25, 133–162.

Govindaraju, K., and Mevelle, G. (1987) Fully automated dissolution and separation methods for inductively coupled plasma atomic emission spectrometry rock analysis. Application to the determination of rare earth elements. Journal of Analytical Atomic Spectrometry, 2, 615–621.

Grew, E.S., and Sandiford, M. (1984) A staurolite-talc assemblage in tourmaline-phlogopite-chlorite schists from northern Victoria Land, Antarctica, and its petrogenetic significance. Contributions to Mineralogy and Petrology, 87, 337–350.

——— (1985) Staurolite in a garnet-hornblende-biotite schist from the Lanterman Range, northern Victoria Land, Antarctica. Neues Jahrbuch für Mineralogie Monatshefte, 9, 396–410.

Griffen, D.T., Gosney, T.C., and Phillips, W.R. (1982) The chemical formula of natural staurolite. American Mineralogist, 67, 292–297.

Hellman, P.L., and Green, T.H. (1979) The high pressure experimental crystallization of staurolite in hydrous mafic compositions. Contributions to Mineralogy and Petrology, 68, 369–372.

Helms, T.S., McSween, H.Y., Jr., Labotka, T.C., and Jarosewich, E. (1987) Petrology of a Georgia Blue Ridge amphibolite unit with hornblende + gedrite + kyanite + staurolite. American Mineralogist, 72, 1086–1096.

Holdaway, M.J., Dutrow, B.L., and Shore, P. (1986) A model for the crystal chemistry of staurolite. American Mineralogist, 71, 1142–1159.

Holdaway, M.J., Dutrow, B.L., and Hinton, R.W. (1988) Devonian and Carboniferous metamorphism in west-central Maine: The muscovite-almandine geobarometer and staurolite problem revisited. American Mineralogist, 73, 20–47.

Irvine, T.N., and Baraggar, W.R.A. (1971) A guide to the chemical classification of the common volcanic rocks. Canadian Journal of Earth Sciences, 8, 523–548.

Maaskant, P. (1985) The iron content and the optic axial angle in zoisite from Galicia, NW Spain. Mineralogical Magazine, 49, 97–100.

Newton, R.C. (1966) Some calc-silicate equilibrium relations. American Journal of Science, 264, 204–222.

Nicollet, C. (1986) Saphirine et staurotide riche en magnésium et chrome dans les amphibolites et anorthosites à corindon du Vohibory Sud, Madagascar. Bulletin de Minéralogie, 109, 599–612.

Parkin, K.M., Loeffler, B.M., and Burns, R.G. (1977) Mössbauer spectra of kyanite, aquamarine and cordierite showing intervalence charge transfer. Physics and Chemistry of Minerals, 1, 301–311.

Perchuk, L.L. (1977) Thermodynamic control of metamorphic processes. In S.K. Saxena and S. Bhattacharji, Eds., Energetics of geological processes, p. 286–352. Springer-Verlag, Berlin.

Perchuk, L.L., Aranovich, L.Ya, Podleskii, K.K., Lavrent'eva, I.V., Gerasimov, V.Yu, Fed'kin, V.V., Kitsul, V.I., Karsakov, L.P., and Berdnikov, N.V. (1985) Precambrian granulites of the Aldan shield, Eastern Siberia, USSR. Journal of Metamorphic Geology, 3, 265–310.

Peucat, J.J., Bernard-Griffiths, J., Gil Ibarguchi, J.I., Dallmeyer, R.D., Menot, P., Cornichet, J., and Iglesias Ponce de Leon, M. (1990) Geochemical and geochronological cross-section of the deep Variscan crust: The Cabo Ortegal high-pressure nappe (northwestern Spain). Tectonophysics, 177, 263–292.

Powell, R. (1985) Regression diagnostics and robust regression in geothermometer/geobarometer calibration: The garnet-clinopyroxene geothermometer revisited. Journal of Metamorphic Geology, 3, 231–243.

Rice, J.M. (1985) Experimental partitioning of Fe and Mg between coexisting staurolite and garnet (abs.). Eos, 66, 1127.

Schreyer, W. (1968) A reconnaissance study of the system MgO-Al_2O_3-SiO_2-H_2O at pressures between 10 and 25 Kb. Carnegie Institution of Washington Year Book, 66, 380–392.

Schreyer, W. (1988) Experimental studies of metamorphism of crustal rocks under mantle pressures. Mineralogical Magazine, 52, 1–26.

Schreyer, W., and Seifert, F. (1969) High-pressure phases in the system MgO-Al_2O_3-SiO_2-H_2O. American Journal of Science, 267A, 407–443.

Schreyer, W., Horrocks, P.C., and Abraham, K. (1984) High-magnesium staurolite in a sapphirine-garnet rock from the Limpopo belt, Southern Africa. Contributions to Mineralogy and Petrology, 86, 200–207.

Seifert, F., and Langer, K. (1970) Stability relations of chromium kyanite at high pressures and temperatures. Contributions to Mineralogy and Petrology, 28, 9–18.

Selverstone, J., Spear, F.S., Franz, G., and Morteani, G. (1984) High-pressure metamorphism in the SW Tauern Window, Austria: P-T paths from hornblende-kyanite-staurolite schists. Journal of Petrology, 25, 501–531.

Smith, D.C. (1984) Remarques cristallochimiques et pétrogénétiques sur des minéraux inhabituels dans les éclogites de Liset et Rekvika, Norvége. 10e Réunion Annuelle Sciences Terre, Bordeaux, p. 511. Société Géologique de France.

Smith, G., and Strens, R.G.J. (1976) Intervalence-transfer absorption in some silicate, oxide and phosphate minerals. In R.G.J. Strens, Ed., The physics of minerals and rocks, p. 583–612. Wiley, London.

Sobolev, N.B., Jr., Kuznetsova, I.K., and Zyuzin, N.I. (1968) The petrology of grospydite xenoliths from the Zagadochnaya kimberlite pipe in Yakutia. Journal of Petrology, 9, 253–280.

Storre, B., and Nitsch, K.-H. (1974) Zur Stabilität von Margarit im System CaO-Al_2O_3-SiO_2-H_2O. Contributions to Mineralogy and Petrology, 43, 1–24.

Ward, C.M. (1984) Magnesium staurolite and green chromian staurolite from Fiordland, New Zealand. American Mineralogist, 69, 531–540.

Willians, H., Turner, F.J., and Gilbert, C.M. (1982) Petrography (2nd edition), 626 p. Freeman and Co., San Francisco.

Manuscript received December 18, 1989
Manuscript accepted December 21, 1990